Scaling and universality of inherent structure simulations

James B. Witkoskie and Jianshu Cao*
Department of Chemistry, Massachusetts Institute of Technology, Cambridge, Massachusetts 02139, USA
(Received 12 November 2003; published 18 June 2004)

In this paper we explore the inherent structures (IS) approach to the dynamics of the East constrained kinetic Ising model. The inherent structures do not capture the nature of the dynamics of many quantities, including the spin autocorrelation function. Simply monitoring the quenched energy fluctuations, i.e., IS energy, results in an oversimplified single order-parameter description of the system's dynamics, but examining other features, such as domain dynamics or normal modes, may give a more complete and useful picture of the dynamics. The universality in the behavior of the IS energy of this model does not reveal nonuniversal features of the kinetics that determine long-time relaxation of the system. As a result, popular functional forms, such as the stretched exponential relaxation or Gaussian distribution of energies, may be a numerical fit to data with little physical justification. Filtering data can be shown to erase features of the system and the resulting quantities resemble more universal functional forms that lack physical insight. These results for the East model have implications for IS simulations of realistic systems and suggest careful analysis including the examination of other potential order parameters is necessary to evaluate the validity of applications of universal and scaling arguments to IS simulations.

DOI: 10.1103/PhysRevE.69.061108 PACS number(s): 64.70.Pf, 61.20.Lc

I. INTRODUCTION

The original inherent structures (IS) concept advanced by Stillinger and co-workers was intended to develop a method of evaluating the partition function of liquids through the use of computer simulations [1]. The goal was to use quenched configurations discovered by simulation, the inherent structures, to partition phase space into basins, and calculate the thermodynamics from these basins. Through the use of clever simulation techniques, the inherent structures would be representative of the most important features of the potential energy landscape and make dominant contributions to partition function. Recent work on IS attempts to extend the IS concept to dynamics by determining the rates of interconversion between various structures or basins [2]. The total rate of interconversion is $O(N)$, where N is the number of rearranging subunits which may be the inherent structures. As a result, one needs to look at the smallest rearranging structures, to capture the physics without having details washed out by competition among subsystems and the IS can play a key role in dynamics [2,3]. In terms of dynamics, the evolution of large complex systems corresponds to motion on a rough multidimensional energy surface with many hills and valleys. Large scale motions on this surface involve overcoming many barriers and require activated dynamics [4]. The IS picture attempts to relate the dynamics of supercooled liquids and glasses to the underlying energy surface and therefore thermodynamics.

The relation between glasses and the IS potential energy landscape is based on the concept of locality. According to Wolynes, on the time scale of experiments, the system cannot find a global minimum of the free energy so the system breaks up into smaller subsystems that minimize the free energy locally. Since these structures are of finite size, the barriers for local rearrangement are finite [5,6]. The objective of many IS simulations is to determine these local structures and the barriers to the local rearrangements [7–14]. The importance of local structures and rearrangements is demonstrated in colloidal systems by Weeks and Weitz and by Cui and Rice [15,16].

The applications of IS to dynamics separate into two groups. One group uses inherent structures to comprehensively extract all information from the system, including the geometry of IS structures and the connectivity, i.e., saddle points between different IS structures [7–12]. The complete information approach also includes determination of normal modes, which have been applied to liquid simulations [3,17–19]. The other applications analyze more universal features in the IS of different systems, such as energy fluctuations [13,14,20]. The latter group uses reduced information to describe the system since universality depends on a few features [13,14,20]. Our analysis of a simple model is an example that the validity of these universal parameters is difficult to establish since the appearance of universality in certain features or quantities may not reflect other important nonuniversal features. Although Stillinger's original IS proposal has profoundly influenced the energy landscape perspective of glass transitions, its connections to simple hopping models, such as the Gaussian trapping model, must be examined with caution.

Several authors recently proposed that the glass phenomenon does not necessarily require the rough potential energy landscape proposed by Stillinger. Through the use of constrained models, such as the Fredrickson-Andersen (FA) constrained kinetic Ising model, they show that the apparent universal features of glasses may be the result of kinetics without any reference to the underlying potential energy landscape [20–25]. Generally, these models have trivial thermodynamics, but complex dynamics. In order to justify the kinetic constraint picture, the constrained models must give

*Electronic address: jianshu@mit.edu

results that are consistent with previous work on IS calculations of model glass forming liquids [26]. Garrahan and coworkers recently performed such analysis [20]. Although they indicate that the important dynamics of this system is governed by large domains of down spins and that IS probes short lived small domains, the relationship between IS dynamics and the domain picture is not conclusive and requires more rigorous exploration.

In this paper we examine the results for IS simulations of the East kinetic Ising model and show that scaling effects as well as the existence of fast and slow processes can explain universal features and functional forms previously reported, while missing important nonuniversal features of the system [20]. These results show that the IS interpretation of this model can be misleading. The fast processes correspond to one and two spin flip events, which is a local rearrangement like those explored by IS on real liquids, but capturing many features of the system, such as the spin autocorrelation function, requires larger scale structures, the domains of down spins [23,24]. Since the East kinetic Ising model has an exponential distribution of length scales with each scale contributing to the overall dynamics, the failure of IS based dynamics to describe the important properties of this model is not surprising. IS generally depends on a well defined length scale so that one can define the smallest structural component or inherent structure of this system [1,3,27]. For sufficiently low temperature liquids one hopes the IS will be representative of the smallest cooperative rearranging regions (CRRs), which dominates the dynamics of liquids [3]. For the kinetic Ising model, CRR is probably a more appropriate definition than IS. This difficulty may not be present in other IS simulations. For example, the FA model dynamics are governed by local structures since a single spin can facilitate its own relaxation so larger scale structures do not influence dynamics as strongly as in the East model. The hierarchy of length scales in the East model makes the simulation sensitive to the choice of system size, temperature, and data filtering. One particular result of the multilength and time-scale nature of this system is that the inherent structures only probe the fastest processes, which may not be the most important features of the system. Choosing a small system size makes the simulation only sensitive to these fast components, while choosing a larger system size can cause trivial scaling effects that obscure the IS physics. As discussed in several references, these features may remain true for other IS simulations since locality is a slightly subjective criterion that can have some ambiguity in computer simulations, which is why much attention has been dedicated to analyzing size effects for these simulations [12]. As a result, the universality interpretation of IS calculations has some ambiguity and requires caution. The universal features of quantities may not reveal important physics and the functional forms generally chosen to fit experimental data, such as the stretched exponential, may not be the result of fundamental physics, but instead result from the flexibility of the functional form or the treatment of simulation data [14,20]. Similar caution about functional forms have been expressed elsewhere [3]. Resolving these ambiguities requires the examination of other potential order parameters.

In the following section, Sec. II, we introduce the East kinetic Ising model and the simulation techniques. These techniques are similar to those applied elsewhere to both the East model and more realistic liquid simulations. This paper uses a very simple model that can be well characterized to better understand the methods applied to more complex systems. In Ref. [28] we use the East model to perform a similar study on mode-coupling closures. After introducing these computational methods, we analyze the fast fluctuations of the East model in Sec. III and slower characteristics in Sec. IV. We show that the fast fluctuations are not well approximated by the stretched exponential reported in other references and that the methods and models used to characterize longer time behaviors are not rigorous [14,20]. To better characterize the system, we discuss a geometrical parameter, the domain sizes, that captures the important properties of the spin autocorrelation function in Sec. V.

II. EAST MODEL AND IS

The East facilitated kinetic Ising model is a chain of spins that take on two values, $n_i=0,1$ [25,26,29,30]. A spin at position i is frozen if the spin to its right is in the down position, $n_{i+1}=0$, but if this spin is in the up position, $n_{i+1}=1$, spin i flips between the up and down position with kinetic rates of $k_{0\to1}=c$ and $k_{1\to0}=(1-c)$. The overall rate of equilibration is unity. The dynamics require spins to move collectively. Since the typical spacing between up spins is on the order of c^{-1}, the system exhibits slow dynamics for small values of c.

The equilibrium distribution of the system is trivial, spins are uncorrelated and $n_i=1$ with probability $P_{up}=c$ and $n_i=0$ with probability $P_{down}=(1-c)$. The lack of correlations implies that there are no interesting features on the potential energy landscape. The thermodynamics correspond to noninteracting spin $\frac{1}{2}$ particles in an external field. For $c<\frac{1}{2}$, we can relate the equilibrium distribution to a temperature, $c/(1-c)=e^{-1/T}$. The model has an ideal glass transition at $T=0$ $(c=0)$ and a mode-coupling transition temperature at $T_c=\infty$ $\left(c=\frac{1}{2}\right)$. Temperatures for $0<c<\frac{1}{2}$ correspond to the energy landscape influenced regime discussed extensively in the literature [13]. Although the thermodynamic landscape is trivial, at any instant in time, the kinetic constraints create an effective landscape by restricting the phase space that is available for the system to explore in a finite observation time. The constraints create valleys of accessible states. Although the states that are not in the valleys are isolated by kinetics, the behavior of the system will be similar to a system with states that are not energetically accessible, i.e., isolated by the potential energy surface. As a result, the effective landscape can resemble a potential energy landscape for short times. From this effective landscape, we define the IS as the lowest energy configuration that is accessible without any activated up spin flipping processes. This configuration corresponds to flipping down all up spins, $n_i=1$, with the $i+1$ neighbor in the up position, $n_{i+1}=1$. The IS energy is the sum of the remaining unflippable spins. This definition of IS ensures uniqueness and avoids effects from the stochastic processes of a zero temperature Monte Carlo simulation.

Figure 1 shows a portion of a time trace of a typical IS trajectory for the East kinetic Ising spin chain with $L=100$

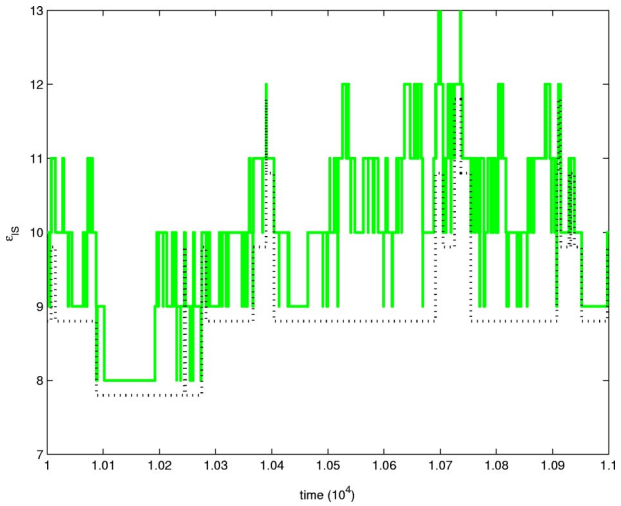

FIG. 1. Typical IS energy simulation for $c=0.10$ and $L=100$. The solid line denotes all observed transitions and the dotted line denotes the IS determined from the energy by filtering the transitions according to the method described in Ref. [13].

spins and $c=0.10$ with periodic boundary conditions. For the lengths chosen in this paper (similar to $5-10c^{-1}$), the simulations show similar behavior for periodic and free boundary conditions. The results for simulations for periodic and free boundary conditions are also similar to monitoring only a fraction of a longer chain, as long as the section of monitored chain is of a comparable length. Monitoring a fraction of a longer spin chain corresponds to having a bath, but since the bath coupling is through a single spin, bath effects are weak. Unfortunately, one cannot couple more realistic IS simulations to a bath as easily. The simulation is performed with kinetic Monte Carlo, where we calculate the rate for all possible flipping processes, k_{ttl}, determine the time of the next transition, $P(t)=k_{ttl}e^{-k_{ttl}t}$, and then choose a spin to flip. We do not consider chains with all down states, so that we can always define k_{ttl}. The omission of the all down state is important since the dynamics of this state is trivial and the state is disconnected from the other states. This simulation method scales with the number of flippable spins, instead of the size of the lattice or time and avoids the effects of discretizing time. These attributes are desirable for simulations with small values of c.

Figure 1 also shows the IS energy determined by using the filtering algorithm designed by Heuer and coworkers [13,14]. Following Heuer's notation, the filtering algorithm labels each distinct IS spin configuration (not energy) visited by the simulation as ξ_i. By comparing configurations, the times of the first occurrence of each IS structure, t_i^*, and the last occurrence of each IS structure, $t_i^\dagger$, are determined. Any two configurations ξ_i and ξ_j with $(t_i^*<t_j^*<t_i^\dagger<t_j^\dagger)$ and $(t_i^\dagger-t_j^*)/\max(t_i^\dagger-t_i^*,t_j^\dagger-t_j^*)<\frac{1}{2}$ are cut by either setting $t_i^\dagger=\max(t,\xi(t)=\xi_i)$ with $t<t_j^*$ or $t_j^*=\min(t,\xi(t)=\xi_j)$ with $t>t_i^\dagger$ (with equal probability). In this expression $\xi(t)$ corresponds to the IS configuration at time t. If the overlap is greater than 50%, $\left[(t_i^\dagger-t_j^*)/\max(t_i^\dagger-t_i^*,t_j^\dagger-t_j^*)>\frac{1}{2}\right]$ the intervals are combined into one IS structure. If $t_i^*<t_j^*<t_j^\dagger<t_i^\dagger$, ξ_j is deleted. The remaining ξ_i do not overlap in time and define the IS metabasins. The time $t_i^\dagger-t_i^\dagger$ is the lifetime of the metabasin and the lowest IS energy encountered during this time interval is the IS energy.

The IS calculation in Fig. 1 resembles the metabasin picture that is seen in many IS calculations on realistic models. The simulation shows fluctuations on many time scales. The short time behavior shows the IS energy fluctuating ±1 around a fairly constant energy before jumping to some other set of values. On the time scale shown in Fig. 1, the system starts with nine up spins and undergoes fluctuations that result in many more up spins (up to 12). Due to the conformational fluctuation, the system is able to enter a different configuration with nine up spins. The energy is the same, but the filtering algorithm ensures that the configuration is different.

A standard interpretation of the time trace is that the fastest fluctuations come primarily from intrabasin motion, while the longer lived fluctuations come from movement between metabasins, but the distinctions between intrabasin and interbasin motion are not well defined for this model since the energy landscape is relatively flat on long length scales (i.e., no metabasins in the potential energy surface). The only features on the landscape are short ranged one and two spin flip barriers. Due to the constrained dynamics, the system cannot explore large regions of the configurational space in a finite time, and a finite simulation of the system appears to have metabasins. As discussed in other references, often Stillinger's notion of a metabasin is replaced by the notion of strongly correlated IS structures, which removes the potential energy from the definition of a metabasin [12,13]. Without large length and energy scale barriers separating metabasins, the distinction of metabasins must be defined relative to time instead of barrier energy. Generally, the simulation time is used to determine the metabasins with the implicit assumption that the time spent in the basins corresponds to the free energy barriers between basins [13,14].

In the following sections we examine different statistics of the East model's IS trajectories, like those in Fig. 1. First we examine the fast processes of the unfiltered data in Sec. III. We find that the fast processes dominate the IS trajectories and most of the contributing processes can be explained in terms of exponential components with possible stretching of some processes attributed to distributions of rate constants and extreme value arguments. It is apparent that the unfiltered data are strongly influenced by the simulation size, which is in some respect arbitrary for this model since the length scales are widely distributed for small values of c. We also show that the stretched exponential fitting of this model in other references does not explain the fundamental physics [20]. In Sec. IV, we explore the filtered data and the appearance of asymptotic agreement with trapping models that have been explored for other systems [14]. The agreement with a model that may have no correspondence with a trapping model may imply that the agreement of simulations with the model may be the result of the filtering algorithm. Section IV also discusses the stretched exponential and its relation to both the filtered and unfiltered IS data. Finally, Sec. V discusses domain dynamics and its ability to capture the long-time dynamics of the East Ising model's single spin correlation function, which occurs on a completely different time scale than the IS dynamics.

III. IS AND FAST PROCESSES

In this section, we examine the IS transition waiting time distribution for the East model, which has also been examined elsewhere [20]. By examining the complete trajectory, we can show that the dominant spin flip processes that change the IS energy for small values of c and L are (i) flipping a down spin between two up spins to the up position, $\uparrow\downarrow\uparrow\rightarrow\uparrow\uparrow\uparrow$, with a corresponding IS trajectory of $\uparrow\downarrow\uparrow\rightarrow\downarrow\downarrow\uparrow$, and energy sequence of $\epsilon_{IS}\rightarrow\epsilon_{IS}-1$; (ii) reversing this flip $\uparrow\uparrow\uparrow\rightarrow\uparrow\downarrow\uparrow$, with IS trajectory $\downarrow\downarrow\uparrow\rightarrow\uparrow\downarrow\uparrow$ and energy sequence $\epsilon_{IS}\rightarrow\epsilon_{IS}+1$; and (iii) flipping the two spins to the left of an up spin to the up position and then flipping the middle spin down $\downarrow\downarrow\uparrow\leftrightarrow\downarrow\uparrow\uparrow\leftrightarrow\uparrow\uparrow\uparrow\rightarrow\uparrow\downarrow\uparrow$ with IS trajectory of $\downarrow\downarrow\uparrow\leftrightarrow\downarrow\downarrow\uparrow\leftrightarrow\downarrow\downarrow\uparrow\rightarrow\uparrow\downarrow\uparrow$ and energy sequence $\epsilon_{IS}\leftrightarrow\epsilon_{IS}\leftrightarrow\epsilon_{IS}\rightarrow\epsilon_{IS}+1$. A two spin flip process where two up spins separated by two down spins makes a transition to a cluster of four up spins decreasing the inherent structures energy is also observed, $\uparrow\downarrow\downarrow\uparrow\rightarrow\uparrow\uparrow\uparrow\uparrow$ with corresponding IS configurations of $\uparrow\downarrow\downarrow\uparrow\rightarrow\downarrow\downarrow\downarrow\uparrow$ and energy sequence of $\epsilon_{IS}\rightarrow\epsilon_{IS}-1$, but it is still a process involving the flipping of two spins. These one and two spin processes account for $>99\%$ of all IS transitions. Processes that involve more spin flips are rare for small values of c since the fast one and two spin flip processes interrupt these slower processes so that only the final stage of the multiple spin process is recognized as an IS transition. The last stage will be recorded as a simple one or two spin flip process.

For low temperatures and small windows, $c=0.05$ and $L=100$, the IS energy probes the three distinct processes. These are the fastest time processes observed and will not be a good indicator of properties influenced by the global features of the system, e.g. the single spin autocorrelation functions. For $c=0.05$ and $L=100$, we expect to have five fairly isolated spins in the up position and most of the dynamics in the IS energy will come from the spins just to the left of these spins as the system jumps between three typical configurations, an isolated spin (or two neighboring up spins), a cluster of three up spins, and two up spins separated by a down spin, $\downarrow\downarrow\uparrow\leftrightarrow\downarrow\uparrow\uparrow\leftrightarrow\uparrow\uparrow\uparrow\leftrightarrow\uparrow\downarrow\uparrow$. As a result, the five spins whose flipping changes the IS energy the most often account for 73% of the IS transitions, 22%, 19%, 15%, 11%, and 7%, respectively, for simulations with 50 000 flipping events, $c=0.05$ and $L=100$. It is important to note that extremely short simulations will be completely dominated by these five spins and infinitely long simulations result in equilibration with all spins contributing equally, but these five spins dominate the IS energy for fairly long simulations. The spins to the right of these hot spins rarely flip since they correspond to the superspins discussed in other references [29].

From Fig. 3, the two single spin processes, $\uparrow\uparrow\uparrow\leftrightarrow\uparrow\downarrow\uparrow$, are easily fit with an exponential waiting time distribution. The exponential form results from the exponential form for the kinetics, the rarity of the starting configurations, and the large time separation of the processes so that these processes do not compete with each other, which would cause mixing of these processes with each other or other slower processes. For small values of c and L the system rarely has more than one single spin up-to-down flipping process available, $\uparrow\uparrow\uparrow\rightarrow\uparrow\downarrow\uparrow$. Specifically, the number of possible processes is approximately Poisson with parameter $\lambda=O(Lc^3)$. Although there is only a 50% chance that the IS transition will take place since there are two possible spin flips ($\uparrow\uparrow\uparrow\rightarrow\uparrow\downarrow\uparrow$ and $\uparrow\uparrow\uparrow\rightarrow\downarrow\uparrow\uparrow$), the rate of this process is $2(1-c)$, which is much faster than the other spin processes. As a result the single exponential waiting time dominates the waiting time distribution for this process. As shown in Fig. 2, the kinetic rate of this process is fairly independent of spin chain size for fairly large spin chains, $L\ll c^{-3}$.

Similar considerations apply for the single spin down-to-up process, $\uparrow\downarrow\uparrow\rightarrow\uparrow\uparrow\uparrow$. For small values of c and L, there are rarely more than one of these single spin configurations, a Poisson with $\lambda=O(Lc^2)$, and the distribution appears to be an exponential. The single spin down-to-up flipping process, $\uparrow\downarrow\uparrow\rightarrow\uparrow\uparrow\uparrow$, is more common than the single spin up-to-down flipping process, $\uparrow\uparrow\uparrow\rightarrow\uparrow\downarrow\uparrow$, and the time-scale separation between the down-to-up process and the fastest two spin processes is not large. As a result, the single spin down-to-up flipping process is much more sensitive to the chain length L. In fact, as shown in Fig. 3 even for $c=0.05$ and $L=100$ there is a small shift in the peak maximum from the expected 1.3 to approximately 1.1 and a slight deviation from an exponential waiting time distribution in the long-time tail. Since the chain length $L=100$ is comparable to c^{-2}, the distortion is not surprising. As shown in Fig. 2, increasing the chain length causes a significant shift in the position of the single spin down-to-up flipping processes and slightly increases deviations from the expected exponential form. Of course in the long chain limit the distribution narrows to a monoexponential again.

The multiple spin processes are multiexponential since they correspond to multiple spin flips and multiple pathways. The most common multiple spin flip transitions are $\downarrow\downarrow\uparrow\rightarrow\uparrow\downarrow\uparrow$, $\downarrow\uparrow\uparrow\rightarrow\uparrow\downarrow\uparrow$, and $\uparrow\downarrow\downarrow\uparrow\rightarrow\uparrow\uparrow\uparrow\uparrow$. The first two processes have triexponential kinetics and the latter process has biexponential kinetics. The processes generally require two slow $O(c^{-1})$ flips resulting in the multiexponential distribution for two spin processes that appear at long times in Fig. 2. The processes are made even slower by the multiple attempts to flip the second spin up before the first spin flips down, for $c=0.05$ the expected time for this process is ≈ 800, which gives a peak at $\log_{10}t\approx 2.9$. The actual peak occurs at a slightly faster time, $\log_{10}t\approx 2.2$ because at any time the fastest process (the extreme value) results in the IS transition. Since we expect approximately five isolated up spins that can contribute to this process, the kinetic rate should be five times faster which gives a peak at $\log_{10}t\approx 2.2$.

The distribution for the multiple spin processes deviates from a sum of a triexponential and biexponential process because of fluctuations in the number of possible two spin processes. Since the number of possible two spin processes will vary more widely than the number of single spin processes, Poisson with $\lambda=O(Lc)$, the distribution will be made wider than the expected multiexponential form. The wider distribution of kinetic rates has been interpreted as stretching [20]. As shown in Fig. 3 the two spin distribution does qualitatively resemble a stretched exponential with $\log_{10}\tau\approx 1.2$ and $\beta_{uwt}\approx 0.44$ [20]. The stretching of the entire distribution

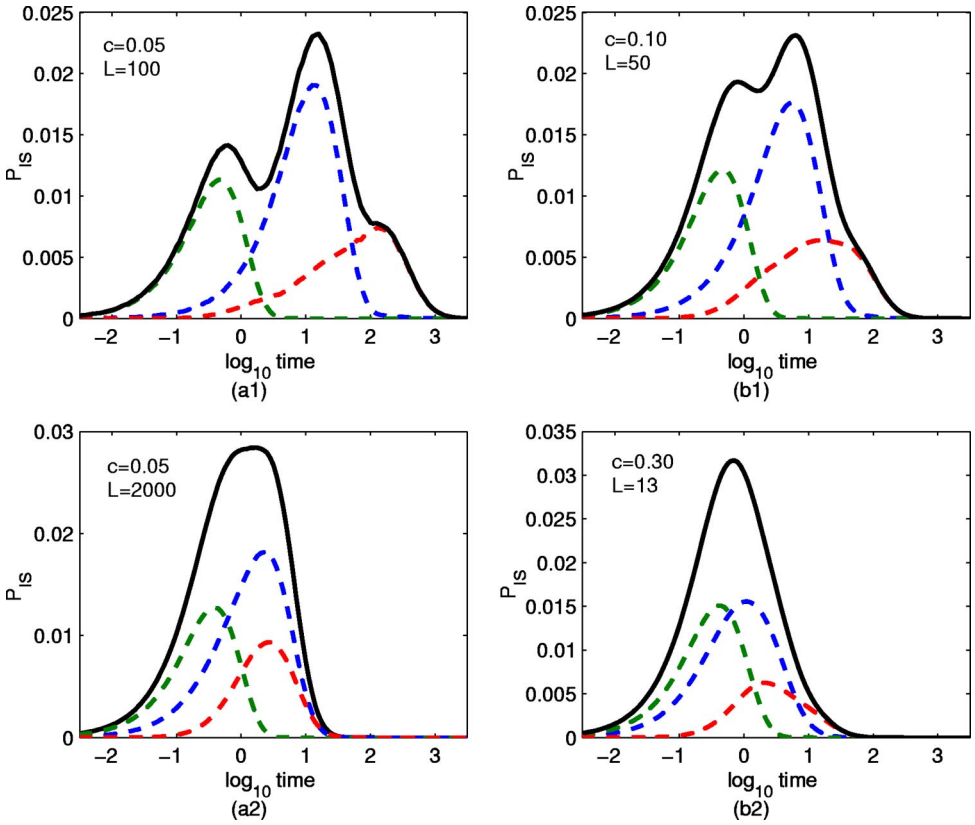

FIG. 2. Log waiting time distribution with time bin size of 0.05 for (a1) $c=0.05$ and $L=100$, (a2) $c=0.05$ and $L=2000$, (b1) $c=0.10$ and $L=50$, and (b2) $c=0.30$ and $L=14$. Solid curves are the total transition probability. The total transition probability can be broken up into three different contributions, as shown by the dashed lines in the figures. The fastest contribution corresponds to a single spin flipping down, $\uparrow\uparrow\uparrow\rightarrow\uparrow\downarrow\uparrow$. The slowest contribution corresponds to processes where two spins flip, $\downarrow\downarrow\uparrow\leftrightarrow\downarrow\uparrow\uparrow\leftrightarrow\uparrow\uparrow\uparrow\rightarrow\uparrow\downarrow\uparrow$ or $\uparrow\downarrow\downarrow\uparrow\rightarrow\uparrow\uparrow\uparrow\uparrow$. The intermediate time contribution corresponds to a single spin flipping up, $\uparrow\downarrow\uparrow\rightarrow\uparrow\uparrow\uparrow$. For $c=0.05$ and $L=100$, the two fastest contributions can be fit with an exponential, and detailed analysis shows that the slowest contribution is close to multiexponential (see text).

is shown in Fig. 4(d) for $c=0.10$ and $L=100$. The original distribution can be fit with a stretched exponential with stretching exponent $\beta_{uwt}\approx 0.36$. Depending on the criterion of the fit, the uncertainty in the exponent can be large. The superexponential falloff makes determination of the actual asymptotics difficult so a more global fit was utilized. The fit is never exceptional with systematic deviations on all intervals, but the short time has the most obvious deviations from the stretched exponential fit.

Extreme value arguments suggest that the stretching will initially increase with L or c since the variation in the number of competing processes increases, but eventually the distribution narrows towards an exponential extreme value distribution as the mean kinetic rate becomes much larger than the width of its distribution. This narrowing results in an approximately exponential distribution of the two spin process for larger lattices as shown in the comparison of Figs. 2(a1) and 2(a2). Increasing c mixes processes and causes deviations from an exponential for the single spin processes as seen in the comparison of Figs. 2(b1) and 2(b2), but the overall distribution narrows towards an exponential since all processes are comparable and extreme value arguments can be applied to the whole distribution. It is important to note that the size of the CRR for the kinetic Ising model is strongly temperature dependent, which is why we must change the lattice sizes for simulations at different temperatures. We have chosen our lattices to have 5 CRRs which is similar to the number seen by Keyes in his simulations, 4.6 CRRs [3]. For the Ising model, the temperature dependence of the size of CRRs is obvious, but the strength of the temperature dependence of the size of CRRs is not clear for more complicated simulations [3,12–14,19]. The narrowing of the waiting time distribution is discussed by Stillinger [1,27]. He argues that the average transition time is inversely proportional to the number of CRRs, and one needs to choose a simulation size that can solvate the IS but only have one CRR. At sufficiently high temperatures, the CRRs may be divorced from the IS so that one may observe an approach to an extreme value or other distribution even though the simulation appears to have a single IS [3].

Extreme value statistics does not completely determine the distribution because of detailed balance. Although the single up-to-down flip process is the fastest process, $\uparrow\uparrow\uparrow\rightarrow\uparrow\downarrow\uparrow$, the system cannot always choose this process because the number of flippable spins will be depleted. Even if the process were available, there is only a 50% chance the system flips this spin before it flips the other spin, $\uparrow\uparrow\uparrow\rightarrow\downarrow\uparrow\uparrow$. As a result the system must perform the single down-to-up spin flips and two spin processes. The need to perform these other processes to maintain detailed balance

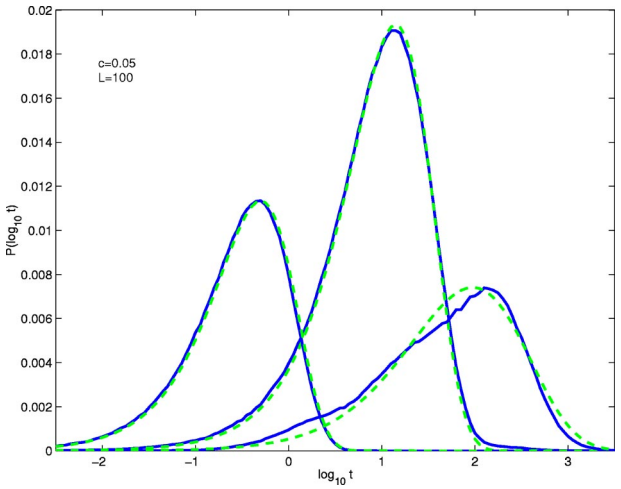

FIG. 3. Individual components of Fig. 2(a1) (solid curves) along with fits to exponentials for the single spin contributions with $\log_{10}\tau \approx -0.3 \approx [2(1-c)]^{-1}$ for the fastest peak, and $\log_{10}\tau \approx 1.1$ for the slower single spin process (intermediate peak). Both fits are within expected binning errors, except for a small long-time tail in the intermediate peak. The two component spin is qualitatively fit with a stretched exponential with $\beta \approx 0.44$ and $\log_{10}\tau \approx 1.2$. The multiple spin processes appear to be a sum of many exponentials and the stretching is the result of declaring that the fit requires too many exponentials.

results in the additional peaks and the nonuniversal behavior of this system.

The detailed balance is not rigorous since more complex processes have a finite chance of occurring, but the predictions are nearly correct for small spin chains. This can be seen by examining the various contributions in Fig. 2. A spin chain with $c=0.05$ and $L=100$ shows 48% of the IS transitions corresponding to the single spin down-to-up flips resulting in a cluster of three up spins, $\uparrow\downarrow\uparrow \rightarrow \uparrow\uparrow\uparrow$, 27% of the IS transitions corresponding to the reverse process $\uparrow\uparrow\uparrow \rightarrow \uparrow\downarrow\uparrow$, and 25% of the IS transitions correspond to two spin processes. Most of the disparity for small values of c can be attributed to an isolated spin transforming to a three up spin cluster just before a different cluster causes an IS transition, $\downarrow\downarrow\uparrow \rightarrow \uparrow\uparrow\uparrow$. If the middle spin of this configuration flips to the down position, $\uparrow\uparrow\uparrow \rightarrow \uparrow\downarrow\uparrow$, this process will be recorded as a fast single spin process. More complex spin processes also make a small contribution to detailed balance violations. As the length of the spin chain increases all of these detailed balance violations from rare events become more probable, which changes these percentages, but even for the $L=2000$ spin chain the percentages changed by 5% as seen by comparing areas in Fig. 2(a1) versus Fig. 2(a2).

The above analysis shows that IS calculations applied to the East facilitated kinetic Ising model only probe the fastest processes of the system. Many of the features of the IS waiting time distribution can be rationalized by labeling different processes. These processes are generally multiexponential. Previous attempts to fit the unfiltered waiting time distribution to stretched exponentials are not very good and come from the distribution of kinetic rates [20]. The size of the simulation is somewhat subjective since the size of CRRs is widely distributed. Choosing a large simulation size $L \gg c^{-1}$ or large value of c results in extreme value arguments determining most of the features of the IS waiting time distribution so that there is a universality caused by a large number of arguments, which may not be important for the physics of

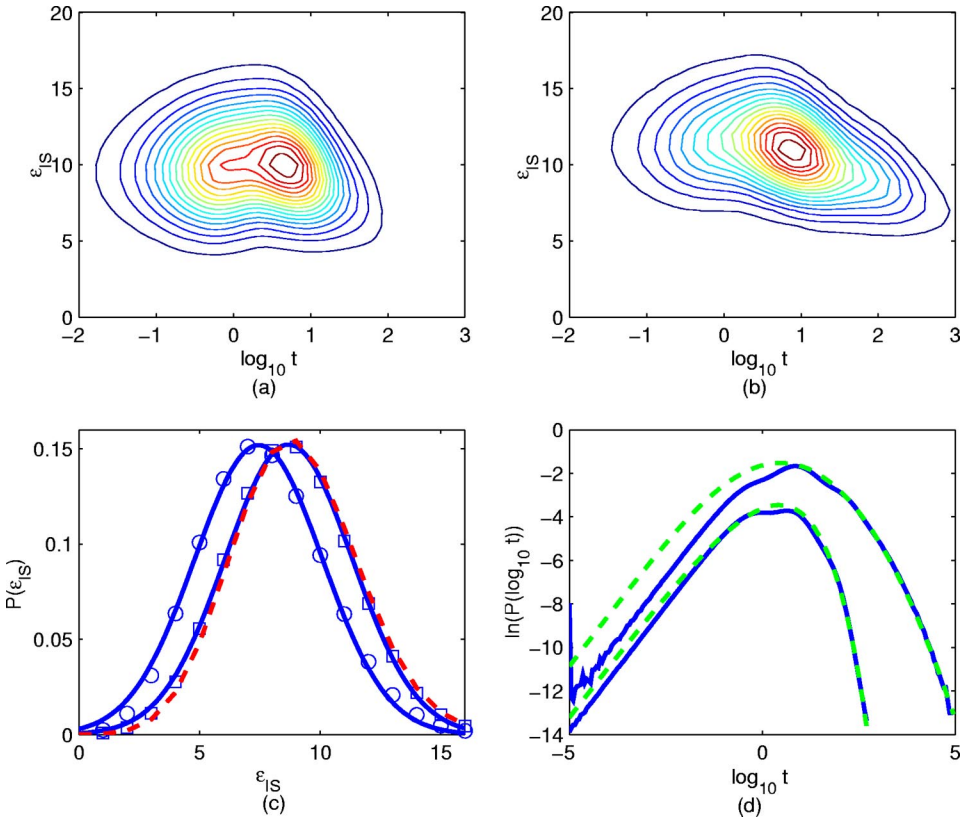

FIG. 4. Contour plot of the waiting time distribution for $c=0.10$ and $L=100$. ϵ_{IS} is an integer and the time bin is 0.05. (a) Shows the unfiltered result. (b) Shows the result with the filtering procedure suggested by Heuer [13]. (c) Shows the resulting probability distribution for the energies at any instant in time along with a Gaussian fit (solid line) and the exact equilibrium IS distribution (dashed line) (□ unfiltered, ○ filtered). The filtering shifted the distribution but did not change the shape significantly. (d) Shows the significant changes in the waiting time distribution caused by the filtering. The upper curves (which were shifted for clarity) correspond to the filtered data (solid line) and the asymptotic Gaussian trapping model fit (dashed line). The lower curves correspond to the unfiltered data (solid line) and a stretched exponential fit (dashed line).

the system. In the following section, we discuss two other apparent universalities that have implication for long-time dynamics, the Gaussian distribution of energies and its relation to the trapping model and the stretched exponential that is fit to many experiments.

IV. TRAPPING MODELS AND IS FILTERING AND SLOW PROCESSES

Previous analysis addresses the role of extreme value arguments on the dynamics of IS trajectories. We now focus on the Gaussian statistics. Using similar arguments about having cL approximately independent regions for short times, the distribution of the IS energies of the system becomes very close to Gaussian as shown in Fig. 4(c) even for fairly short chain lengths, $c=0.10$ and $L=100$. This size avoids finite size effects for the domain dynamics discussed in the following section. Figure 4(a) shows a contour plot of the IS waiting time distribution as a function of IS energy and Fig. 4(b) shows the same information with filtering defined in Ref. [13]. The plot in Fig. 4(a) clearly shows features such as a double peak that would not be consistent with the predictions of a Gaussian trapping model or exponential extreme value statistics [14,31]. Reducing the information by calculating the time independent IS energy probability results in a distribution that can be easily fit with a Gaussian as shown in Fig. 4(c). The figure also shows that filtering changes the peak position, but it does not significantly alter the width of the distribution. Since the equilibrium IS energy results from Bernoulli random variables, the Gaussian form is not entirely surprising as shown by the exact unfiltered equilibrium IS energy calculation also presented in Fig. 4(c).

Unlike the equilibrium properties, the dynamics of the system are affected significantly by the filtering, as shown in Fig. 4(d). The unfiltered IS waiting time distribution is multipeaked, but applying the filtering algorithm proposed by Heuer and coworkers results in a distribution with a single peak. As discussed earlier and demonstrated in Fig. 1, Heuer's algorithm selects both long lived structures and quasitransition states that are stable against one or two spin flips. If two structures differ by only a single spin flip and the simulation spends a long time in either structure, the simulation is likely to flip flop between them and the filtering algorithm will consider them to be in the same metabasin. Achieving a transition to another metabasin generally requires the system to make several flips so that it is entropically difficult to return to the same basin, and the intermediate configurations will be recorded at short lived metabasins.

As shown in Fig. 4(d), the log waiting time distribution of the longer lived structures asymptotically resembles the Gaussian trapping model prediction in the long-time limit, $P(\log(t)) \sim e^{-\ln(t/\tau_0)^2/\Delta^2}$, where $\Delta^2=(\beta E_0)^2$ where E_0 is supposed to correspond to the width of the equilibrium distribution, $P(\epsilon_{IS}) \propto e^{-(\epsilon_{IS}-\epsilon_{IS}^0)^2/E_0^2}$. Unfortunately, the Δ^2 values from $P(\log(t))$ is four times smaller than the prediction from the measured equilibrium distribution. Similar disparities are reported for simulations on Lennard-Jones systems [14]. The Gaussian trapping model's waiting time distribution can also be approximated by a stretched exponential [31].

Generally, a stretched exponential that fits the data goes to zero much faster than either the simulation data or the trapping model. The deviation occurs asymptotically and the function would be near zero at the point of deviation, so any noise will hide the effect. The accuracy of the fit with the trapping model to the asymptotics (long time) is high over many orders of magnitude, but it is not clear why this system should follow the Gaussian trapping model. It is important to note that the asymptotics are independent of simulation length for long simulations, but obviously not infinite simulations since the system is ergodic and the space is finite dimensional (one metabasin). Shorter simulations result in a sharper cutoff. Possibly the filtering algorithm, which uses coin flipping statistics to separate basins and combines basins based on an arbitrary 50% overlap criterion sufficiently erases details to achieve this scaling law.

For $c=0.10$ and $L=100$ in Fig. 4, the unfiltered data can also be fit with a stretched exponential as discussed above, but the fit is not asymptotically as accurate as the Gaussian trapping model fit to filtered data [20]. The best fit to the asymptotics of the unfiltered waiting time distribution is with stretched exponent $\beta_{uwt} \approx 0.36$, but there is a large uncertainty caused by the definition of the asymptotic regime since this function goes to zero quickly on a logarithmic scale. This unfiltered waiting time exponent β_{uwt} is close to the stretching exponent determined by fitting the unfiltered IS correlation function, $[\langle \epsilon_{IS}(t)\epsilon_{IS}(0)\rangle - \langle \epsilon_{IS}(0)\rangle^2]/[\langle \epsilon_{IS}^2(0)\rangle - \langle \epsilon_{IS}(0)\rangle^2]$. The fit to the correlation function with exponent $\beta_{ucf}=0.39$ is good as long as one ignores systematic deviation in the residuals [20]. Other simulations on realistic simulations have reported fits with no systematic deviations in the residuals so the stretched exponential may still be valid for other systems but not the East model [3]. The IS correlation function and fit are shown in Fig. 5. In fact, the fit to the waiting time distribution with $\beta_{ucf}=0.39$ is comparable to the fit with $\beta_{uwt}=0.36$. Similarly, the Gaussian trapping model's prediction for approximate stretching with exponent $\beta_{gwt}=[1+\frac{1}{2}\Delta^2]^{1/2}=0.43$ is close to the asymptotic stretching of the filtered correlation function $\beta_{fcf}=0.47$. The Δ value is determined from the asymptotics of the waiting time distribution instead of the energy distribution, $P(\log(t)) \sim e^{-\ln(t/\tau)^2/\Delta^2}$ [14,31]. Once again there is a disparity between the prediction with $\Delta=\beta E_0$ and the IS energy correlation function. The filtered IS correlation function exponent β_{fcf} is measured from the dashed line in Fig. 5. The fit is only in the last two decades that can be calculated accurately, because a small correlation function will make the $\ln[-\ln(C(t))]$ sensitive to fluctuations in $C(t)$. In this regime, there are no systematic deviations in the residuals of the fit. As always, fits on $\ln[-\ln(C(t))]$ versus $\ln(t)$ plots should be suspect since many variations will be washed out.

The agreement between the exponents for the waiting time distribution and the correlation function is possible since the long-time relaxation in the correlation function should be dominated by the slowest IS jumps, which are determined by the tail of the waiting time distribution. Since there is no reason for the trapping model to be valid for the East model, the resulting disparity between the static IS en-

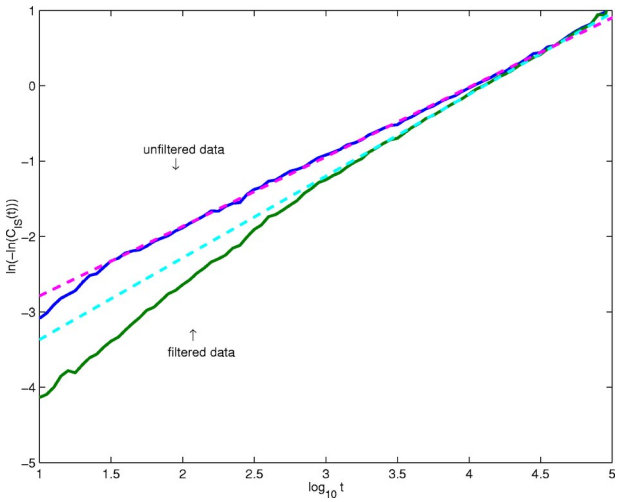

FIG. 5. The IS correlation function, $\langle \epsilon_{IS}(t)\epsilon_{IS}(0)\rangle - \langle \epsilon_{IS}(0)\rangle^2 / \langle \epsilon_{IS}(0)^2\rangle - \langle \epsilon_{IS}(0)\rangle^2$, for both the filtered data (lower solid curve) and the unfiltered data (upper solid curve). The two distributions approach each other at long times. The lower dashed curve shows the long-time stretched exponential fit to the filtered data with $\beta_{fcf}=0.47$, which is close to the prediction based on the waiting time distribution in Fig. 4, $\beta_{gwt}=0.43$. The upper dashed curve shows a short time fit to the unfiltered data with $\beta_{ucf}=0.39$, which is in close agreement to the fit in Fig. 4, $\beta_{uwt}=0.36$. As always, one must view double log vs log plotted data with incredulity.

ergy distribution and both the IS energy correlation function and the IS waiting time distribution is not surprising. The fact that the trapping model can be used at all is much more surprising, and shows that the result may come from the filtering algorithm and not the physics of the system [14].

Figure 5 shows that both the unfiltered and filtered correlation functions asymptotically approach the stretched exponential with $\beta_{ucf}=0.47$. This asymptotic approach results in the systematic deviations in the fit of the unfiltered data to the stretched exponential with exponent $\beta_{ucf}=0.39$. As mentioned above, the escape from apparent metabasins should dominate long-time relaxation of both filtered and unfiltered simulations so the long-time agreement is expected. At short times, the unfiltered data decay more quickly since fast fluctuations are not removed. The IS energy correlation function has a small tail at times that are much longer than the filtered IS waiting time distribution. This tail would not be present in the trapping model since all correlations are lost once an IS transition occurs.

The Gaussian trapping model's log waiting time distribution only resembles a Gaussian asymptotically, $\ln[P(\log_{10}t)] \propto \log_{10}t^2$, as shown by the Gaussian trapping model fit in Fig. 4(d). The fit performed in this figure is an exact numerical calculation, but the asymptotics are consistent with the Gaussian form reported in several references [14,31]. The distribution of traps must asymptotically behave as a Gaussian to get the asymptotic behavior in the waiting time. In fact, the central region of the waiting time distribution of this model does not resemble a Gaussian. Most sums of random variables deviate from a Gaussian in the tails of the distribution not the center. This phenomenon has been observed in the experiments of Sakurai and coworkers, where an exponential tail in the distribution of trapped electrons in thermoluminescence studies was hidden by a broader Gaussian distribution before cleaning the surface [32,33].

V. DOMAINS AND DYNAMICS

Since the IS picture of East model is very sensitive to temperature and size effects and the apparent fits to various functional forms are questionable in some respects, a more complete picture is necessary. As has been suggested, but not fully explored in some of the references, a possible strong measure of the dynamics of this system, or dynamical heterogeneity, is the lifetimes of clusters of down spins [23,24,29]. Below we will show that the dynamics of the single spin correlation function is very well approximated by domain dynamics.

Domains have been defined as the size of a cluster of adjacent down spins, or the distance between the nearest two up spins. For small values of c, the domains can be quite large. Since eliminating a domain requires a process that must flip each down spin to the up position for a short period of time, larger domains are generally much longer lived than smaller domains. The domain picture is also supported by the superspins discussed above [29]. We define the lifetime of a domain as the time when the spin on the left side of the domain flips to the down position. This spin can only flip when the domain to its right has vanished. Figure 6 shows two-dimensional plots of the lifetimes of domains. The vertical axis corresponds to the size of the domain at $t=0$. This initial probability follows the trivial equilibrium initial conditions, $P(n)=c(1-c)^n$. The horizontal axis refers to $\log_{10}t$. The high peaks at short times correspond to disappearance of small domains. These peaks are sharp because there is a dominant sequence of spin flips to remove these spins. As n increases, more paths become available resulting in a broader and more smeared distribution of lifetimes. As c decreases, the number of domains that have a dominant path determining their lifetime increases, resulting in more peaks. The small c picture is consistent with the analysis of Sollich and Evans, who assume a time-scale separation in domain lifetimes [29]. The fluctuations in the smallest domains were sampled by the IS calculations presented above. As shown in Fig. 6, increasing c significantly shortens the lifetimes of domains. For domains of size $n \ll c^{-1}$, the average domain lifetimes follow the predictions of Sollich and Evans, $\tau_n \sim n^{1/T \ln 2}$, but the lifetimes are much faster for $n \approx c^{-1}$. This result has been discussed by Sollich and Evans. For sufficiently long domains, an entropic consideration does not require the use of the lowest path, which was originally assumed in their derivation [29].

The time scales of the lifetimes of the domains are significantly longer than the time scales for the inherent structure calculations. The differences in the time scales are demonstrated in Figs. 6(a2) and 6(b2), which compares the lifetime of a single domain with the unfiltered IS waiting time distribution. The filtering algorithm does not increase the waiting time distribution enough to become comparable to the domain lifetime [see Fig. 4(d)], but the IS correlation

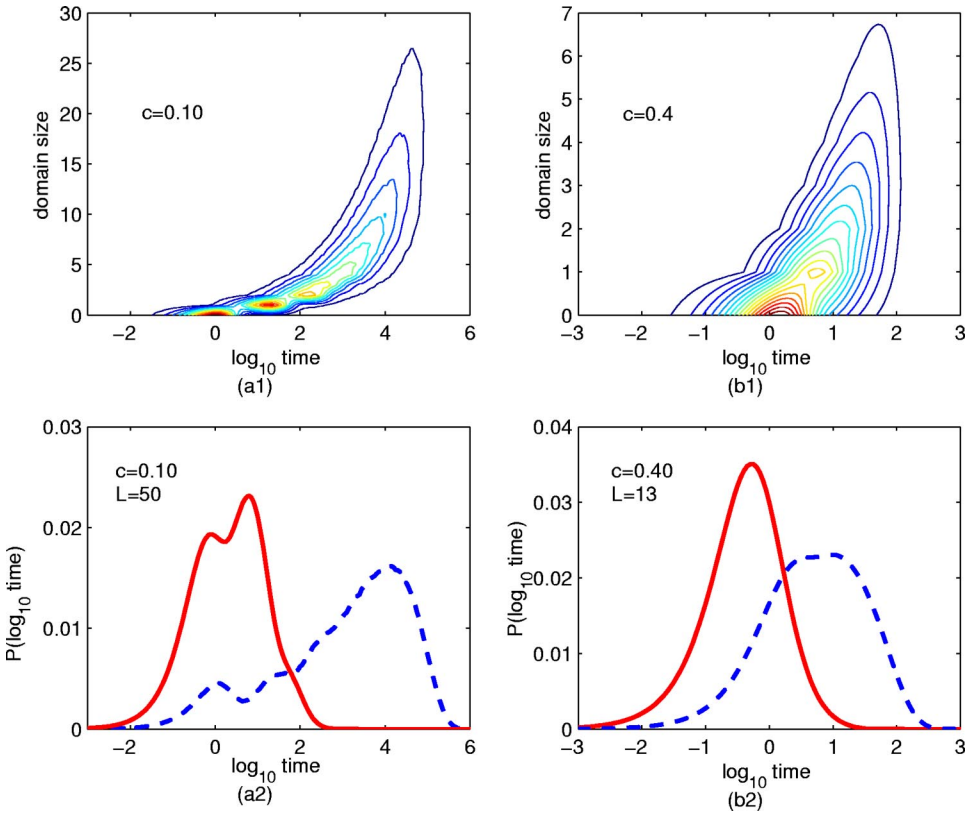

FIG. 6. The domain lifetimes as a function of size for (a1) $c=0.10$ and (b1) $c=0.40$. The time bin size is 0.05. (a2) and (b2) compare the waiting time distribution determined from the domain lifetimes (dashed curves) against IS calculations presented in Fig. 2 (solid curves) with (a2) $c=0.10$ and $L=50$ and (b2) $c=0.40$ and $L=13$. These quantities capture different physics of the system.

function has a small tail that has a time scale that is similar to the domain dynamics time scale (see Fig. 5). No functional relationship between domain dynamics and this small tail in the IS energy correlation function is apparent, but the similar time scales are not surprising since the relaxation of superspins will play a role in the relaxation of IS energy.

For small values of c, one expects the single spin correlation function to be primarily determined by the lifetime of the domain to the right of that spin. This result can be understood because once a spin's right neighbor is in the up position, it will equilibrate with a unit rate. For small values of c, the equilibration with unit rate is a much faster process than the time of the domain dynamics so domain dynamics are the rate limiting steps. Figure 7 shows the single spin correlation function, $C(t)=[\langle n_i(t)n_i(0)\rangle - c^2]/(c-c^2)$, versus the integrated domain lifetime probability function, $1-\Sigma_l \int dt P(t|l)P(l)$. The single spin correlation function has recently been calculated by combining mode-coupling and asymptotic analysis [28]. For $c>0.20$, the domain lifetime is sufficiently short that the time scales for equilibration and the domain lifetime are of the same order so that the comparison is not satisfactory for short times although the two quantities agree asymptotically since there is always a small contribution from larger domains. For smaller values of $c=0.10$ and 0.05, the required time separation between the disappearance of the domain and the equilibration of a spin with a neighbor are sufficiently large so that the approximation is very accurate, even for small values of time. Cicerone and Ediger experimentally studied similar time separation of global and local relaxation [34]. The agreement between these predictions for the spin relaxation shows that spatial considerations are necessary in the analysis of this model. These spatial considerations are not well captured by the inherent structure energy calculations.

VI. CONCLUSION

The East model and other related kinetically constrained models have stimulated interest in the theoretical community because of the simple construction and rich dynamics. These

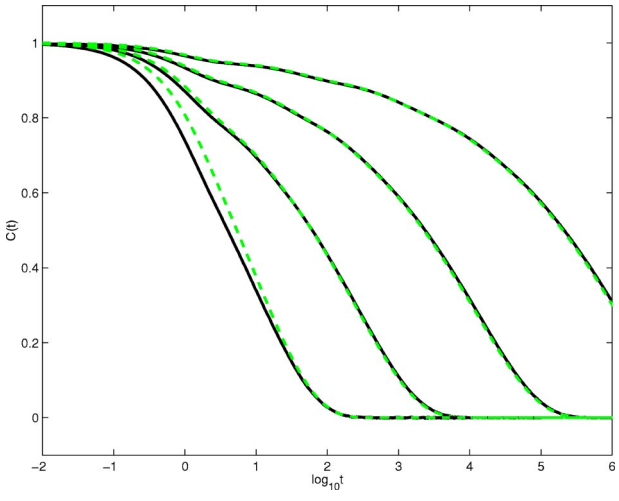

FIG. 7. The single spin correlation function, $[\langle n_i(t)n_i(0)\rangle - c^2]/(c-c^2)$ (solid curve), vs the prediction for the domain lifetime, $1-\Sigma_l \int dt P(t|l)P(l)$ (dashed curve). The corresponding values of c in order from bottom to top are $c=0.40$ (bottom curve), $c=0.20$, $c=0.10$, and $c=0.05$ (top curve). Slight discrepancies at long times are the artifact of the time binning interval 0.05.

models' explicit connection to realistic systems and predictive power remain elusive. In this paper we used the East model as a simple example to calibrate IS dynamics. We also investigate mode-coupling closures of this model in Ref. [28]. The insight gained from this research helps us to understand the tools that are applied to the study of dynamic slow-down and glass phenomenology. These studies identify strengths and weaknesses of these methods, which can help us to improve them, but the specific scaling relations and mode-coupling closures are not directly transferable to realistic systems.

Studies of IS dynamics show that landscapes and possibly configurational entropy concepts need to be defined with respect to a time scale or characteristic energy or temperature since an important quantity in defining dynamics is the free volume in phase space that is currently available to the system. Including time allows us to treat kinetic constraints and energetic considerations on the same footing so that we can examine the IS dynamics of the East model. Scaling laws or other standard functional forms can be misleading as shown by both the apparent stretched exponential and universal forms displayed by the East model. Although these concepts are important for systems with universality, the existence of the universality for the model needs to be more rigorously established.

Apparent universality may be the result of the examined quantities failing to be good order parameters because the description of the system with these order parameters is overreduced. The universality of a particular parameter may not reflect a universality in the interesting physics of the system or can result from simulation details that have no physical meaning, such as filtering. The filtering causes the observed transitions to correspond to the sum of many processes, which improves the legitimacy of a large number of arguments, but does not help to reveal the underlying physics in this model. For the East kinetic Ising model, the IS energy was too reduced of a description, but including the domain size and—to a lesser extent–examining IS configurations, which are geometrical parameters, captures the important long-time physics. Although the results and methods will be system specific, rigorous methods and detailed analysis of IS is necessary to validate any universality conclusions from IS based dynamic methods.

ACKNOWLEDGMENTS

This research was supported by AT&T and the NSF.

[1] F. H. Stillinger and T. A. Weber, Phys. Rev. A **25**, 978 (1982).
[2] F. H. Stillinger and T. A. Weber, Phys. Rev. A **28**, 2408 (1983).
[3] T. Keyes and J. Chowdhary, Phys. Rev. E **65**, 041106 (2002).
[4] C. A. Angell, Y. Z. Yue, L. M. Wang, J. R. D. Copley, S. Borick, and S. Mossa, J. Phys.: Condens. Matter **15**, S1051 (2003).
[5] X. Xia and P. G. Wolynes, Proc. Natl. Acad. Sci. U.S.A. **97**, 2990 (2000).
[6] X. Xia and P. G. Wolynes, Phys. Rev. Lett. **86**, 5526 (2001).
[7] J. P. K. Doye and D. J. Wales, Science **271**, 484 (1996).
[8] D. J. Wales, Science **271**, 926 (1996).
[9] N. Giovambattista, F. W. Starr, F. Sciotino, and S. V. Buldyrev, Phys. Rev. E **65**, 041502 (2002).
[10] F. W. Starr, S. Sastry, J. F. Douglas, and S. C. Glotzer, Phys. Rev. Lett. **89**, 125501 (2002).
[11] S. Sastry, P. G. Debenedetti, F. H. Stillinger, T. B. Schroder, J. C. Dyre, and S. C. Glotzer, Physica A **270**, 301 (1999).
[12] S. Buchner and A. Heuer, Phys. Rev. E **60**, 6507 (1999).
[13] B. Doliwa and A. Heuer, Phys. Rev. E **67**, 031506 (2003).
[14] R. A. Denny, D. R. Reichman, and J. P. Bouchaud, Phys. Rev. Lett. **90**, 025503 (2003).
[15] E. R. Weeks and D. A. Weitz, Phys. Rev. Lett. **89**, 095704 (2002).
[16] B. Cui and R. Rice, J. Chem. Phys. **114**, 9142 (2001).
[17] J. P. Stoessel and P. G. Wolynes, J. Chem. Phys. **80**, 4502 (1984).
[18] J. S. Cao and G. A. Voth, J. Chem. Phys. **103**, 4211 (1995).
[19] J. Chowdhary and T. Keyes, Phys. Rev. E **65**, 026125 (2002).
[20] L. Berthier and J. P. Garrahan, J. Chem. Phys. **119**, 4367 (2003).
[21] G. H. Fredrickson and H. C. Andersen, Phys. Rev. Lett. **53**, 1244 (1984).
[22] G. H. Fredrickson and H. C. Andersen, J. Chem. Phys. **83**, 5822 (1985).
[23] J. P. Garrahan and D. Chandler, Proc. Natl. Acad. Sci. U.S.A. **100**, 9710 (2003).
[24] J. P. Garrahan and D. Chandler, Phys. Rev. Lett. **89**, 035704 (2002).
[25] F. Ritort and P. Sollich, Adv. Phys. **52**, 219 (2003).
[26] A. Crisanti, F. Ritort, A. Rocco, andM. Sellitto, J. Chem. Phys. **113**, 10 615 (2000).
[27] F. H. Stillinger, Abstr. Pap. - Am. Chem. Soc. **216**, 482 (1998).
[28] J. Wu and J. S. Cao (unpublished).
[29] P. Sollich and M. R. Evans, Phys. Rev. Lett. **83**, 3238 (1999).
[30] S. Eisinger and J. Jackle, J. Phys. A **26**, 7325 (1993).
[31] C. Monthus and J. P. Bouchaud, J. Phys. A **29**, 3847 (1996).
[32] T. Sakurai and R. K. Gartia, J. Appl. Phys. **82**, 5722 (1997).
[33] T. Sakurai, K. Shoji, K. Itoh, and R. K. Gartia, J. Appl. Phys. **89**, 2208 (2001).
[34] M. T. Cicerone and M. D. Ediger, J. Chem. Phys. **103**, 5684 (1995).